

Temperature Effects and Resonance Elastic Cross Section Influence on Secondary Energy Distributions of Scattered Neutrons in the Resolved Resonance Region

V.V. Kolesov, V.F. Ukraintsev
Obninsk Institute of Nuclear Power Engineering
249040 Studgorodok 1, Obninsk, Kaluga reg., Russia

Abstract

It is customary to neglect the effect of thermal motion (Doppler effect) and resonance behavior of elastic cross section on the energy distribution of scattered neutrons in the resonance region. But as has been shown earlier for ^{238}U , there is certain effect of replacing usual step-function by more exact expression, where σ_s has resonance behavior

The question of interest was to check the effect of replacing step distribution by more exact one for the simplest cylindrical two-zone cell with different V_{mod} / V_f . A code has been written to solve slowing-down equation from unit source in ultra-fine energy scale with two different kernels. Energy averaged cross sections were calculated for ^{238}U and ^{235}U .

KEYWORDS: elastic scattering distribution function, slowing-down equation, cell calculations

It is customary to neglect the effect of thermal motion (Doppler effect) and resonance behavior of elastic cross section on the energy distribution of scattered neutrons in the resonance region. But as has been shown in [1-4] for ^{238}U , there is certain effect of replacing usual step-function

$$\sigma_s(E')f_s(E' \rightarrow E) = \begin{cases} \frac{\sigma_s(E')}{(1-\alpha)E'}, & \alpha E' \leq E \leq E' \\ 0, & E > E', E < \alpha E', \end{cases} \quad (1)$$

where $\alpha = (A-1)^2 / (A+1)^2$,

for the energy distribution of scattered neutrons in the resolved resonance region by more exact expression:

$$\sigma_s(v')f_s(v' \rightarrow v) = \frac{1}{v'} \int_{-1}^1 \int_0^\infty v_r \sigma_s(v_r) g(\vec{v}' \rightarrow \vec{v}) 2\pi P(V) d\mu dV, \quad (2)$$

where \vec{v}' , \vec{v} - initial and final velocities of neutron in laboratory system, V - initial velocity of the nucleus in laboratory system before the collision, v_r - relative velocity of the neutron and the nucleus before the collision

$$v_r^2 = v'^2 + V^2 - 2v'V\mu; \quad \mu = \cos(\vec{v}' \bullet \vec{V}),$$

$$g(\vec{v}' \rightarrow \vec{v}) = \begin{cases} \frac{2v}{v_{\text{max}}^2 - v_{\text{min}}^2}, & v_{\text{min}} \leq v \leq v_{\text{max}} \\ 0, & v \leq v_{\text{min}}, v \geq v_{\text{max}} \end{cases},$$

where v_{min} , v_{max} is

$$v_{\text{min}} = \left| V_c - \frac{A}{A+1} v_r \right|, \quad v_{\text{max}} = \left| V_c + \frac{A}{A+1} v_r \right|,$$

V_c – velocity of the center of mass,

$$P(V) - \text{Maxwellian distribution, } \int_0^{2\pi} P(V) d\mu dV d\varphi = 2\pi P(V) d\mu dV,$$

φ – azimuthal angle between \vec{v}' and \vec{V} .

When σ_s suppose to be a constant in (2), we can get well known monoatomic gas model with *erf* – functions. As had been shown in [1-2], integral (2) could be simplified and numerically calculated.

We have also found certain differences between calculations of the energy distribution of scattered neutrons as (1) and (2) for all significant nuclei, as ^{240}Pu , ^{167}Er , ^{155}Gd , ^{238}U and ^{235}U .

Figure 1: Elastic scattering distribution function for the 38 eV resonance of ^{240}Pu for $T=210\text{K}$ and incident energy $E'=37.9344\text{ eV}$.

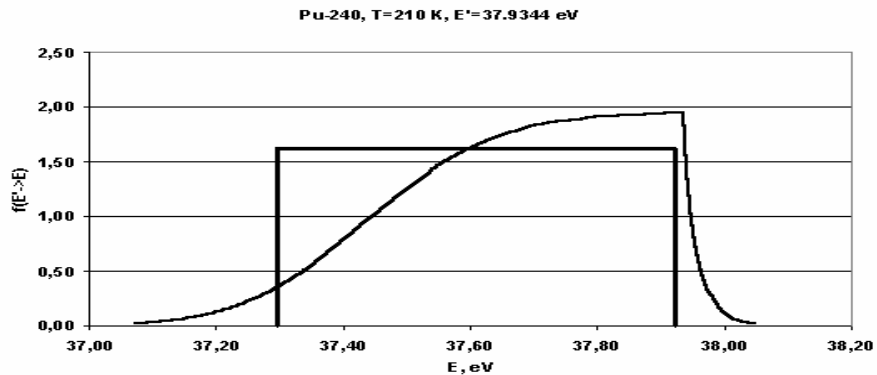


Figure 2: Elastic scattering distribution function for the 38 eV resonance of ^{240}Pu for $T=1200\text{K}$ and incident energy $E'=37.9344\text{ eV}$.

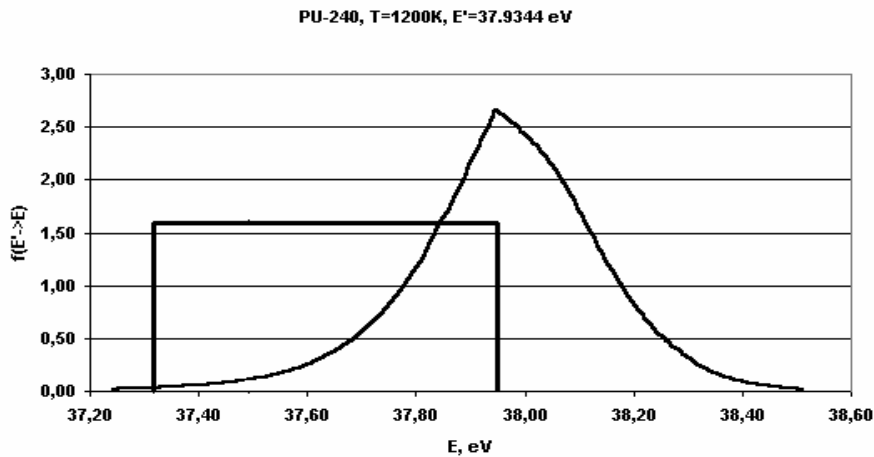
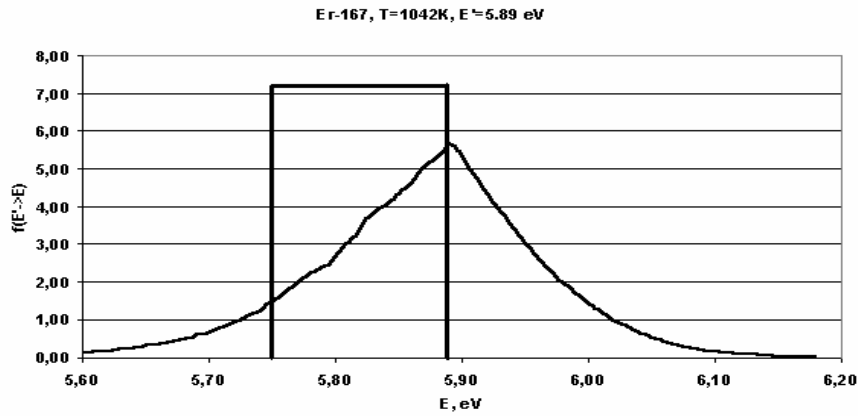


Figure 3: Elastic scattering distribution function for the 5.98 eV resonance of ^{167}Er for $T=1042\text{K}$ and incident energy $E'=5.89\text{ eV}$.



As an example, figs.1-3 gives us the energy distribution of scattered neutrons $f_s(E' \rightarrow E)$, as function of E , for certain E' for ^{240}Pu ($T=210\text{K}$ and 1200K), and also for ^{167}Er , when $T=1042\text{K}$.

The question of interest was to check the effect of replacing distribution (1) by distribution (2) as a function of V_{mod} / V_f for the simplest cylindrical two-zone cell. A code has been written to solve slowing-down equation from unit source in ultra-fine energy scale with kernel (1) and (2) for this cell.

We have taken the following cell specifications.

Atomic number densities ($\times 10^{24} \text{ 1/cm}^3$):

fuel (1042K): $^{238}\text{U} - 0.0224228,$
 $^{235}\text{U} - 0.0007652,$
 $^{16}\text{O} - 0.0441;$

moderator (600K): $\text{H}_2\text{O}.$

Geometry: $R_{\text{fuel}} = 0.4098 \text{ cm},$
 $R_{\text{mod}} = 0.61781 \text{ cm}$ (cell 1, $V_{\text{mod}} / V_f = 1.273$),
 $R_{\text{mod}} = 0.5 \text{ cm}$ (cell 2, $V_{\text{mod}} / V_f = 0.489$),
 $R_{\text{mod}} = 0.7 \text{ cm}$ (cell 3, $V_{\text{mod}} / V_f = 1.918$),

To check this code we have also compared resulting microscopic ^{238}U cross sections with Monte-Carlo calculations.

Table 1: Comparison of microscopic ^{238}U cross sections in the energy range 35.5 – 37.0 eV for cell 1.

Value	Model (2)	Model (1)	Difference (%)	Monte-Carlo (error, %)
$\langle \sigma_t \phi \rangle / \langle \phi \rangle$	193	160	20.6	152 (1.0)
$\langle \sigma_s \phi \rangle / \langle \phi \rangle$	103	84	22.6	80 (1.0)

Table 2: Comparison of microscopic ^{238}U cross sections in the energy range 35.5 – 37.0 eV for cell 2.

Value	Model (2)	Model (1)	Difference (%)	Monte-Carlo (error, %)
$\langle\sigma_t\phi\rangle/\langle\phi\rangle$	169	138	22.5	135 (1.0%)
$\langle\sigma_s\phi\rangle/\langle\phi\rangle$	89	72	23.6	70 (1.0%)

Table 3: Comparison of microscopic ^{238}U cross sections in the energy range 35.5 – 37.0 eV for cell 3.

Value	Model (2)	Model (1)	Difference (%)	Monte-Carlo (error, %)
$\langle\sigma_t\phi\rangle/\langle\phi\rangle$	204	170	16.7	160 (1.0%)
$\langle\sigma_s\phi\rangle/\langle\phi\rangle$	109	90	17.4	84 (1.0%)

Table 4: Comparison of microscopic ^{235}U cross sections in the energy range 35.5 – 37.0 eV for cell 1.

Value	Model (2)	Model (1)	Difference (%)	Monte-Carlo (error, %)
$\langle\sigma_t\phi\rangle/\langle\phi\rangle$	70.5	73.1	3.6	74.6 (1.3)
$\langle\sigma_s\phi\rangle/\langle\phi\rangle$	17.7	17.9	1.1	18.0 (1.2)

Table 5: Comparison of microscopic ^{235}U cross sections in the energy range 35.5 – 37.0 eV for cell 2.

Value	Model (2)	Model (1)	Difference (%)	Monte-Carlo (error, %)
$\langle\sigma_t\phi\rangle/\langle\phi\rangle$	72.3	75.4	4.1	76.7 (1.3)
$\langle\sigma_s\phi\rangle/\langle\phi\rangle$	17.8	18.0	1.1	18.1 (1.2)

Table 6: Comparison of microscopic ^{235}U cross sections in the energy range 35.5 – 37.0 eV for cell 3.

Value	Model (2)	Model (1)	Difference (%)	Monte-Carlo (error, %)
$\langle\sigma_t\phi\rangle/\langle\phi\rangle$	69.8	72.3	3.5	74.5 (1.2)
$\langle\sigma_s\phi\rangle/\langle\phi\rangle$	17.6	17.8	1.1	17.9 (1.1)

Tables 1 – 6 presents the differences in microscopic ^{238}U and ^{235}U cross sections in the energy range 35.5 – 37 eV (around ^{238}U resonance) for model (1) and (2). We can also see that model (1) calculations are close to Monte-Carlo ones and rather differences from model (2) calculations. To explain this result we must take into account, that only simple thermalization monoatomic gas model when σ_s suppose to be a constant realized in

present Monte-Carlo codes, which don't take into account resonance behavior of neutron scattering cross sections.

Conclusion

It has been shown that resonance neutron elastic cross section essentially influence on secondary energy distributions of scattered neutrons in the resolved resonance region. This effect depends from resonance parameters and cell V_{mod} / V_f value. For example, effect of replacing distribution (1) by the exact one for total and elastic scattering microscopic ^{238}U and ^{235}U cross sections is more essential when $V_{\text{mod}} / V_f = 1.273$ rather than when $V_{\text{mod}} / V_f = 0.5$. It needs additional studies to determine when this effect must be taken into account for neutron multigroup constant calculations. We are planning to check effect described above for ^{239}Pu and ^{240}Pu in cells with MOX fuel also. It's very interesting to incorporate this model into NJOY code as suggested in [5] and investigate this effect with more precise method.

Acknowledgements

This project is supported by RFFI, grant № 05-08-65467-a

References

- 1) G.L. Blackshaw, R.L. Murray. Scattering Functions for Low-Energy Neutron Collisions in a Maxwellian Monoatomic Gas. Nucl. Sci. Engng., 27, 520-532 (1967).
- 2) A.Yu. Kurchenkov, N.I. Laletin. Neutron-Scattering Indices at Moving Monoatomic-Gas Nuclei in the Resonance Energy Region. Atomnaya Energiya, 70, 368-372 (1991).
- 3) M. Ouisloumen, R. Sanchez. A Model for Neutron Scattering Off Heavy Isotopes That Accounts for Thermal Agitation Effects. Nucl. Sci. Engng., 107, 189-200 (1991).
- 4) O. Bouland, V. Kolesov, J.L. Rowlands. The Effect of Approximations in the Energy Distributions of Scattered Neutrons on Thermal Reactor Doppler Effects. Proc. Int. Conf. on Nucl. Data for Science and Technology, Gatlinburg, USA, 1994, 1006-1008, (1994).
- 5) W. Rothenstein. Proof of the formula for the ideal gas scattering kernel for nuclides with strongly energy dependent scattering cross sections. Ann. Of Nucl. Energy. 31, 9-23 (2004).